



Received on 30 April 2023; received in revised form, 23 June 2023; accepted 04 July 2023; published 01 December 2023

## FORMULATION AND EVALUATION OF CURCUMIN-LOADED CHITOSAN NANOPARTICLES AND ITS INTRANASAL EFFICACY FOR CNS DELIVERY

Lucky Mangal<sup>\*</sup>, Nitin Kaushik and Sanjar Alam

Department of Pharmaceutics, R. V. Northland Institute, Greater Noida - 203207, Uttar Pradesh, India.

### Keywords:

Curcumin, Nanoparticles, Chitosan, Tripolyphosphate, Intranasal delivery

### Correspondence to Author:

**Lucky Mangal**

Assistant Professor,  
Department of Pharmaceutics,  
R. V. Northland Institute, Greater  
Noida - 203207, Uttar Pradesh, India.

**E-mail:** luckymangal47@gmail.com

**ABSTRACT:** Hydrophobic medications that are taken orally having poor bioavailability due to permeability issues. They experience a chemical and enzymatic breakdown in the digestive system and exhibit a significant amount of hepatic first-pass metabolism. Similar obstacles prevent the development of effective therapeutic molecule delivery systems and the discovery of new drugs. It has been revealing that curcumin, a key active lipophilic constituent of *Curcuma longa* (Zingiberaceae), has a variety of pharmacological properties, including cholagogues, anticancer, and anti-inflammatory properties. Based on its organoleptic characteristics, solubility, loss on drying, partition coefficient, infrared spectroscopy, and differential scanning calorimetry, Curcumin was physically and chemically characterized. The drug sample Curcumin was found to be genuine and pure based on the tests. For the purpose of determining *in-vitro* release and permeation study, an analytical method utilizing RP-HPLC was created and validated. Ionic gelation was used to create chitosan nanoparticles. The study includes the evaluation of various processing conditions, including surface morphology, particle size, particle size distribution, surface charge, percentage yield, entrapment efficiency, and drug loading, as well as *ex-vivo* permeation studies and *in-vitro* release models. For Curcumin-nanoparticles, the impact of drug concentration on particle size, polydispersibility index, entrapment efficiency, and loading capacity was optimized. It was found that as the drug: polymer ratio is raised; the average size of curcumin-loaded nanoparticles grows. As per ICH guidelines, the formulation's stability study was also carried out.

### INTRODUCTION:

**Curcumin:** Turmeric is generated from curcumin (*Curcuma longa*- Haldi). Curcumin, like many herbal therapeutic compounds, was first ingested as a portion of food before being shown to have a significant pharmacological effect.

It has been used as a muscle relaxant and anti-inflammatory drug in Ayurveda (Indian school of medicine) for years to reduce inflammation and pain in the skin and muscles. It has also been shown to have melanoma effects.

Curcumin is revered in traditional Indian medicine as a "body purifier," and science is discovering a growing list of sick disorders that can be remedied by turmeric's bioactive constituents<sup>1</sup>. It may represent involvement in Alzheimer's disease pathogenesis anti-inflammatory and anti-capabilities. In Monocytic THP-1 cells, Curcumin diminishes an induced Egr-1 production of proteins

	<b>QUICK RESPONSE CODE</b> <b>DOI:</b> 10.13040/IJPSR.0975-8232.14(12).5916-29
	This article can be accessed online on <a href="http://www.ijpsr.com">www.ijpsr.com</a>
<b>DOI link:</b> <a href="https://doi.org/10.13040/IJPSR.0975-8232.14(12).5916-29">https://doi.org/10.13040/IJPSR.0975-8232.14(12).5916-29</a>	

and Egr-1 DNA-binding activity. The significance of Amyloid peptide-induced cytochemokines gene expression in monocytes is mediated by Egr-1 was already studied. Curcumin lowers inflammation *via* inhibiting Egr-1 DNA-binding function. Curcumin inhibits monocyte chemotaxis, which can be initiated by chemokines secreted by stimulated microglia and astrocytes inside the brain. Curcumin appears to be a significant inhibitor of pro-inflammatory cytokine production in these trials, although this may vary depending on the nature of the target cells <sup>2</sup>.

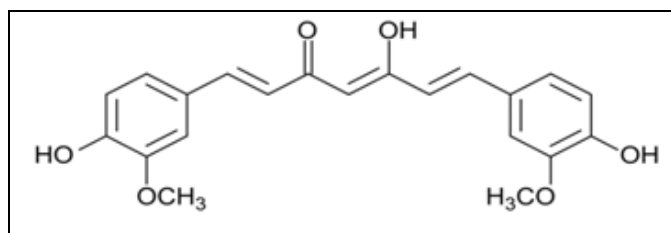


FIG. 1: CHEMICAL STRUCTURE OF CURCUMIN

**Chitosan:** Chitosan is a natural polymer *i.e.*, an N-deacetylated peptide that is a duplicate of chitin found in crustaceans, insects, fungus, and other organisms. Several fascinating properties of chitosan have been found, including the ability to form films, gelation capabilities, bio adhesion properties, and permeation-increasing effects, which are explained by opening epithelial cell tight intersections. Chitosan is also a polymer *i.e.*, biodegradable and biocompatible that has attracted a lot of interest in the pharma industry, in addition to food science and cosmetic applications, due to its promising qualities. It has been converted into nanoparticles (NPs) and microparticles for the encapsulation of biological and pharmaceutical substances <sup>3</sup>.

Due to its cationic nature as a polymer, CS has the ability to interact with molecules or polymers that are negatively charged. Recently, cationic chitosan and anionic counter ions like TPP have been used to create chitosan microparticles or nanoparticles through ionic interaction. Nanoparticles and microparticles are formed by flocculation of the Chitosan polymer in this known as the ionic gelation process. Ionic reaction should allow the cationic chitosan molecule in these particulate gel beads to bind anionic compounds. As a result, it is easy, harmless, and requires aqueous phases mixing at room temperature.

This approach of producing drug-containing chitosan nanoparticles without the use of organic solvents has received a lot of attention. IR spectra, X-ray photoelectron spectroscopy, and velocimetry were utilized in separate articles to confirm the interaction or binding of opposite charged molecules of CS NP's. The release profiles of CS NPs made using this technology revealed a high explosive effect within 1/2 hour and a rapid entire release of the drug. This behavior indicates that chitosan's with an ionic reaction may have weak binding capabilities and that chitosan's are not the best excipients in the formulation, as evidenced by the literature <sup>4</sup>.

Nasal vaccine delivery using these nanoparticles were also investigated. The anti-tetanus IgG levels and anti-tetanus IgA titers elicited by tetanus toxoid-loaded nanoparticles were higher than those induced by solution vaccinations at 6 months following injection. The electrostatic attachment of drug-loaded molecules to the cationic CS polymer explains the carrier and stabilizer effect. Because of polymers have large mol. weight (70-150 kD) demonstrated an adverse immunogenic reaction following parenteral administration, commercially made chitosan can't be used for parenteral preparations <sup>5</sup>.

**Nanoparticles:** According to the history of development process, as novel challenges arise with greater size, their solutions must be determined at a level far deeper than previously recognized. From macroscale (>1 mm) to microscale (100–0.1 mm) to nanoscale (100–0.1 nm), now we have a better knowledge of science and technology (100-1 nm). With the introduction of biotech drugs, such as proteins, DNA, and RNA molecules, which can alter disease pathophysiology, the need for new drug delivery technology is pressing to overcome the size and stability issues associated with these new drugs, as well as to design methods to deliver these drugs in a controlled manner <sup>6</sup>.

Drug nanoparticles are drug-containing particles with a diameter of less than 1 $\mu$ m. These isolated and submicron-sized particles have been used for a different type of purposes, including targeted drug administration, controlled release, and increased bioavailability of water-insoluble medicines.

The goal of modern drug therapy is to improve the pharmacological properties of medications while reducing their negative side effects. Colloidal drug carriers that enable targeted drug delivery or site-specific delivery in a magic-bullet concept while ensuring optimum drug release profiles are a good choice. The most extensively studied colloidal carriers have been liposomes and nanoparticles. Polymeric nanoparticles have been proposed as an alternative drug carrier because liposomal formulations have some technological constraints, such as poor stability and limited drug entrapment effectiveness<sup>7</sup>.

Polymeric nanoparticles (which act as drug carriers/ reservoirs) or nanosuspensions of the active therapeutic agent (which are made using various milling or homogenization methods to enhance the surface area and thus the solubility, dissolution, and bioavailability of insoluble drugs) are 2 types of nanoparticles used in drug delivery. For the manufacture of drug nanoparticles, a number of materials have been used, including biodegradable (e.g., PLGA, PLA, PGA, etc.) and non-biodegradable (e.g., sodium alginate, chitosan, etc.) pharmaceutically appropriate polymers. For the objectives of this study, representative polymers of both categories were utilized as model polymeric materials<sup>8</sup>.

#### METHODS AND MATERIAL:

**Materials:** They also (Bangalore, India) provided chitosan and TPP with deacetylation degrees of 85% and average molecular weights of 40 kDa. Sigma-Aldrich supplied PVA (87-90% hydrolyzed, average molecular weight 30,000- 70,000 Da), dichloromethane, and sucrose Steinheim, Germany. The curcumin was provided by the Dabur Research Foundation, India, through Sigma Chemical Company. MERCK supplied absolute grade ethanol from Changshu Hongsheng Fine Chemical Co., Ltd., India). Fisher Scientific provided HPLC quality acetone from RFCL Limited, India. IOL Chemical Ltd. (Mumbai, India) supplied GAA, while potassium dihydrogen phosphate and methanol were supplied by S.D. Fine Chemicals, Ltd. (Mumbai, India).

**Solubility Determination:** The Curcumin solubility was measured in distilled water and phosphate buffer with a pH of 7.4. To test the drug

solubility, 25 ml of each solvent was separated from the excess curcumin and placed in separate conical flasks. In a mechanical shaker, the flasks were sealed and clamped. The shaker bath was set to a temperature of 25°C. Samples were taken in every 24 hours until equilibrium was attained (72 hrs.). Shimadzu UV-1601 was used to record absorbances after the samples were filtered and diluted (Shimadzu, Kyoto, Japan)<sup>9</sup>.

**Melting Point Determination:** Curcumin was reduced in size to a very fine powder and dried at temperatures much below its melting point. It was then inserted into a glass capillary tube. A sufficient amount of dry medication powder was used to create a compact column with a height of 4-6 mm. This capillary tube, together with the thermometer, was then placed into the HICON melting point apparatus (Ningbo Hicon Industry Co. Ltd, Zhouxiang, China). The temperature at which the drug melted was recorded<sup>10</sup>.

**Analytical Methodology:** For the preliminary and *in-vitro* research of curcumin, the reported HPLC and UV-spectrophotometric method was validated. As part of a typical research effort, a new HPLC method was refined and validated, and its application in plasma analysis was tested<sup>11</sup>.

**UV Spectroscopy:** To determine the  $\lambda_{\max}$ , 100 mg Curcumin was diluted in 100 ml of distilled H<sub>2</sub>O and scanned by the UV spectroscopy in the range of 200-800 nm.

**Preparation of Calibration Curve in PBS with pH 7.4:** To generate a 1 mg/ml stock solution, 50 mg of Curcumin dissolved in 50 ml of phosphate buffer with pH 7.4. Stock solution (1000 g/mL) was serially diluted at concentrations ranging from 2-20 g/ml, and absorbance was measured at 425 nm by using a Shimadzu UV-1700 instrument (Shimadzu, Kyoto, Japan). As a blank, a double beam spectrophotometer was used with phosphate buffer (pH 7.4). A graph was plotted between absorbance (y-axis) and concentration (x-axis)<sup>12</sup>.

**Fourier Transform Infrared Spectroscopy:** The FT-IR technique is used to get the infrared spectrum of absorption or emission of a gas, solid, or liquid. FT-IR spectrophotometer collects the data with a large spectral range with high spectral resolution.

This is a very important advantage over a dispersive spectrophotometer, which is limited in its ability to detect intensity over a limited range of wavelengths at once. The process of transform raw data into a spectrum using a (Perkin Elmer) Fourier- Transform is referred to as Fourier Transform Infrared Spectroscopy (mathematical strategy)<sup>13</sup>.

**DSC:** Using a DSC Q2000 (TA Instruments, New Castle, USA) fitted with the TA Universal Analysis 2000 software, a thermogram of curcumin nanoparticles was obtained. Each sample was set inside a T- zero aluminum pan, covered with a T-zero cover, and studied at 10°C/min. scan rate between 30 and 350°C. A 50 mL/min. nitrogen stream was used to run the samples through an empty reference pan<sup>14</sup>.

**HPLC Method for Curcumin:** The HPLC was validated for *in-vitro* analysis in PBS at pH 7.4.

**HPLC Requirements:** A reverse phase Phenomenex column C<sub>18</sub> (25 cm × 4.6, or 5 μm) with a mobile phase of water, methanol, and 2-propanol (50:45:5 v/v) and a flowing rate is 1 ml/min were used to analyze the samples. The drug eluted after 10 minutes, and its amount was detected spectrophotometrically at 425 nm.

**Curcumin Calibration Curves Prepared using the HPLC Method:**

**Instrumentation:** Shimadzu HPLC with UV detector attached.

**Column:** Phenomenex C<sub>18</sub> reversed - Phase column (Particle size 5 μm, 25 cm x 4.6 mm).

**Mobile Phase:** Water: Methanol: 2-propanol.

**Flow Rate:** 1 ml/min.

**Detection:** 425 nm, UV detection.

**Retention Time:** 7.34 ± 0.1 min.

**Injection:** 20 μL.

Curcumin stock solution of 0.1 mg/mL was made by diluting 10 mg drug with 100 mL of methanol. From the stock solution (100 g/mL), serial dilutions for concentration ranging from 2-20 g/mL were prepared. A graph was drawn showing the relationship between the area under the curve (y-axis) and concentration (x-axis). A Calibration curve of Curcumin was created using the HPLC technique for drug content estimation and *in-vitro* study. **Fig. 6** depicts a representative HPLC chromatogram of the drug<sup>15</sup>.

**Formulation Development:**

**Ionic Gelation Method:** Chitosan was used as a mucoadhesive polymer. The Chitosan nanoparticles were created by the ionic gelation method with tripolyphosphate anions. For this experiment, CS was dissolved in glacial acetic acid (2% v/v) at different concentration (0.05, 0.1, 0.15, 0.175, 0.2, 0.25 and 0.3% w/v). TPP was dissolved in distilled H<sub>2</sub>O at concentrations of 0.1, 0.15, 0.2, and 0.3% w/v. Finally, 4 ml of TPP solution was dropped into 10 mL of CS solution and stirred at room temperature for 30 min. Visual examination of the samples revealed three distinct systems: aggregates, opalescent suspension (nanoparticles), and clear solution. The particles in an opalescent suspension are very tiny, in the nano range. Opalescent suspensions (nanoparticles) were chosen from the preparations with various concentrations of chitosan and TPP, and their mean particle sizes were determined<sup>16</sup>.



**FIG. 2: FORMULATION DEVELOPMENT OF CURCUMIN- LOADED CHITOSAN NANOPARTICLES**

**Characterization of Placebo NPs:** The mean size, polydispersibility index (PDI), and zeta potential of the nanoparticles was determined by the zeta sizer (Nano ZS 90, Malvern, UK). Curcumin-chitosan

nanoparticle characterization was examined using a TEM (JEM-3011, JEOL, Tokyo, Japan) and an SEM (JSE- 5200, JEOL, Tokyo, Japan)<sup>17</sup>.

**Preparation of Drug-loaded Chitosan Nanoparticles:** Curcumin was incorporated into the nanoparticles by combining the drug with chitosan solution and storing the solution for 24 hrs. To obtain nanoparticles, the TPP was added drop wise to the drug-containing chitosan solution while stirring after 24 hrs.

**Determination of Nanoparticle Encapsulation Efficiency, Loading Capacity, and Percentage Yield Determination:** The encapsulation efficiency and loading capacity of nanoparticles were revealed by ultracentrifugation at 14000 rpm for 45 minutes at 4°C from an aqueous medium containing non- associated Curcumin. The amount of free Curcumin in the supernatant was determined using a UV spectrophotometer set to 425 nm. The encapsulation efficiency (EE) and loading capacity (LC) of Curcumin NP's were calculated using the formulae provided below and all measurements were performed in triplicate<sup>18</sup>.

$$EE = (\text{Total drug} - \text{Free drug}) / (\text{Total drug}) \times 100$$

$$LC = (\text{Total drug} - \text{Free drug}) / (\text{Nanoparticles weight}) \times 100$$

The percentage yield was determined as the total dry weight of initial materials ( $W_2$ ) and the weight of dried NP's recovered ( $W_1$ ) as:

$$\text{Percentage yield (\%)} = W_1 / W_2 \times 100$$

**Evaluation of Developed Formulation and their Optimization:**

**Dynamic Light Scattering is used to Determine Particle size:** DLS measurements were taken with a Nanosizer 90ZS to measure the size distribution and average size of the polymeric micelles (Malvern Instruments, Southborough, MA). The intensity of dispersed light was measured in relation to an incident beam at 90°C. After filtering the micellar aqueous solution with a membrane extruder with a pore size of 0.2 mm, the freeze-dried powder was dispersed in an aqueous buffer, and measurements were taken (Millipore, St Charles, MO). All of the data analysis was done automatically. The size that was measured was displayed as the mean of 20 runs with three measurements taken during each run<sup>19</sup>.

**Zeta Potential:** At 25°C, the zeta potential of chitosan nanoparticles was calculated using a Zeta Plus Zeta Potential Analyzer (Brookhaven, USA). The samples were adjusted to pH 4.5 with 0.1 mM NaCl solution and automatically monitored to maintain a consistent ionic strength. Each sample was measured 3 times, and the values shown are the average of 2 replicate samples<sup>20</sup>.

**Surface Morphology of Drug-loaded Chitosan Nano-particles by TEM:** By using TEM, the surface morphology and size of the generated nanoparticles were determined. The nanoparticle was given one minute to adhere to the carbon substrate after being dropped a drop of nanosuspension onto a paraffin sheet. The remaining drug suspension was eliminated by adsorbing the drop on the corner of some filter paper. Following that, the grid was left on the phosphotungstate drop for 10 sec. The sample was air dried after filter paper was used to absorb any remaining liquid. The sample was studied by TEM (Morgagni 268D TEM, Massachusetts, USA)<sup>21</sup>.

**In-vitro Release Study:** Using the dialysis method, the in-vitro release of curcumin from the curcumin solution was calculated. 40 mL of PBS containing 0.1% Tween-80 were used to dissolve 4 mL of each formulation in a dialysis bag (MWCO 3500 Da). A 100-rpm swirl was applied to the dialysis bag at 37°C. 1 mL of the sample was taken out and the same volume of fresh media was added at the predetermined intervals (0.25, 0.5, 1, 2, 4, 6, 8, 24, 48, and 72 hrs.). The HPLC technique was used to determine the concentration of curcumin<sup>22</sup>.

**Ex-vivo Nasal Permeation Study:** Skin attaches to the cell body (receptor) and cell cap (donor). The shot of isotonic saline solution was given through a specially designed passageway. The lower part of the water jacket surrounding the isotonic saline solution chamber receives temperature-controlled water, which circulates out through the upper part to ensure a constant temperature of 32°C. A Teflon-coated magnetic bar provides agitation and promotes uniform distribution of temperature throughout the saline bathing solution.

A syringe is used to withdraw the sample, and the drug content is determined using a UV spectrophotometer. The receptor cell was filled

with medium, and 1 ml of nanoparticle was applied to the skin surface of donor compartment. The receptor media was kept at  $35.5 \pm 0.5^\circ\text{C}$  and agitated magnetically at 600 rpm. After the test formulation was applied to the donor side, 0.5 ml of an aliquot was taken from the receiver cell at specified intervals (*i.e.*, 0, 1, 2, 3, 4, 5, 8, 10, 12 and 24 hrs.) for a period of 24 hrs and immediately replaced with the same amount of fresh media maintained at  $35 \pm 0.5^\circ\text{C}$ . The samples were filtered through a 0.45 m membrane filter after the necessary dilutions, and the amt. of drug in the receptor medium was determined using a UV spectrophotometer at 425 nm<sup>23</sup>.

**Data Analysis:** Measurement and plotting the rate of curcumin permeation through the skin ( $Q$ ,  $\text{g}/\text{cm}^2$ ) as a function of time (hrs.) was carried out. The drug flux at steady state was calculated using the slope of the linear component of the curve ( $J_s$ ,  $\text{g}/\text{cm}^2/\text{hr}$ ) (Misra *et al.*, 2016)

Cumulative amount of drug permeated = (Concentration ( $\mu\text{g}$ )  $\times$  Volume of diffusion cell) / (Area ( $\text{cm}^2$ ))

Volume of diffusion cell = 20 ml

Area of diffusion cell =  $3 \text{ cm}^2$

Flux = Slope of steady-state portion of the cumulative amount of drug permeation v / s time ( $\mu\text{g}/\text{cm}^2/\text{hrs.}$ )

Permeability coefficient ( $P_b$ ) = Flux / (Drug concentration in donor compartment ( $\mu\text{g}/\text{ml}$ ))

Drug concentration in donor compartment ( $C_d$ ) = 20  $\mu\text{g}/\text{ml}$ .

## RESULTS:

### Solubility Record:

**TABLE 1: CURCUMIN'S SOLUBILITY DATA WERE AS FOLLOWS**

Medium	Solubility
Water	Sparingly soluble
Methanol	Soluble
Ethanol	Soluble
Acetonitrile	Readily soluble
Ethylacetate	Readily soluble
Hexane	Sparingly soluble

Curcumin is freely soluble in methanol, insoluble in water, readily soluble in ethyl acetate and acetonitrile and sparingly soluble in hexane.

### Melting Point Determination:

#### DSC:

**TABLE 2: MELTING POINT OF CURCUMIN FOUND AS FOLLOWS**

Reported melting point	183°C
Observed melting point	189°C

Curcumin was discovered to have a melting point of 189°C. This value approximates the 183°C value mentioned in the literature.

### Analytical Data:

#### Calibration Curve of Curcumin:

**TABLE 3: WAVELENGTH OF CURCUMIN**

Solvent	$\lambda_{\text{max}}$
Ethanol/Methanol	425 nm

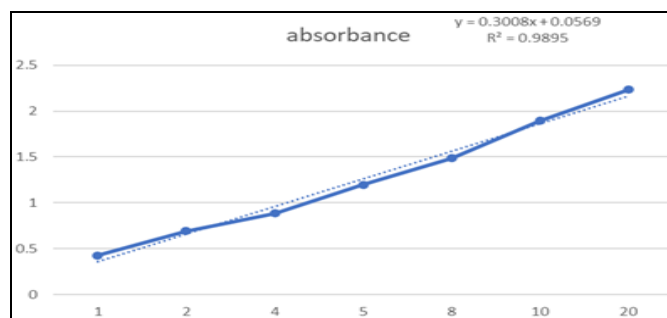


**FIG. 3: CALIBRATION CURVE OF CURCUMIN**

### FTIR Spectra of Curcumin showing Characteristics Band and Stretching:

IR spectra of curcumin Fig. 4 display stretching vibrations at around  $1628 \text{ cm}^{-1}$ , primarily attribute to the overlapping stretching vibrations of alkenes ( $\text{C}=\text{C}$ ) and carbonyl ( $\text{C}=\text{O}$ ).

### FTIR Spectrum:

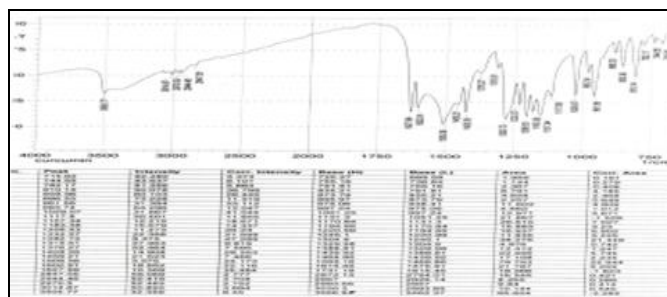


**FIG. 4: FTIR SPECTRA OF CURCUMIN**

The ligands IR spectrum exhibits stretching vibrations caused by O- groups at  $3200\text{-}3500 \text{ cm}^{-1}$ ,  $\text{C}=\text{C}$  aromatic stretching vibration at  $1427 \text{ cm}^{-1}$ , and a high intensity band at  $1512 \text{ cm}^{-1}$  that includes mixed vibrations of stretching carbonyl bond vibrations ( $\text{C}=\text{O}$ ) and in- plane bending vibrations around aliphatic  $\text{CC}-\text{C}$ ,  $\text{CC}=\text{O}$ .

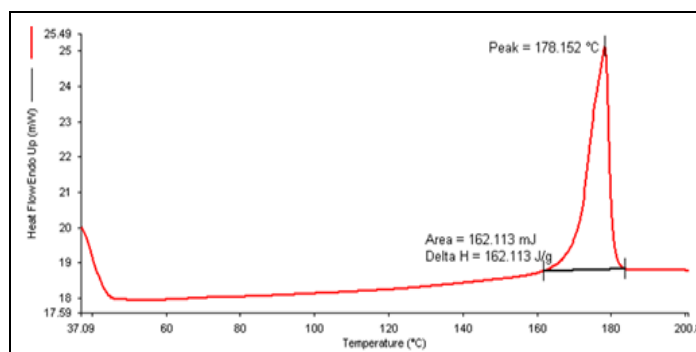


FIG. 5: DSC ANALYSIS OF CURCUMIN

Fig. 5 displays Curcumin DSC thermograms. The drug showed an endothermic peak at 178.152°C and the melting point of Curcumin is 183°C according to literature citation.

HPLC:

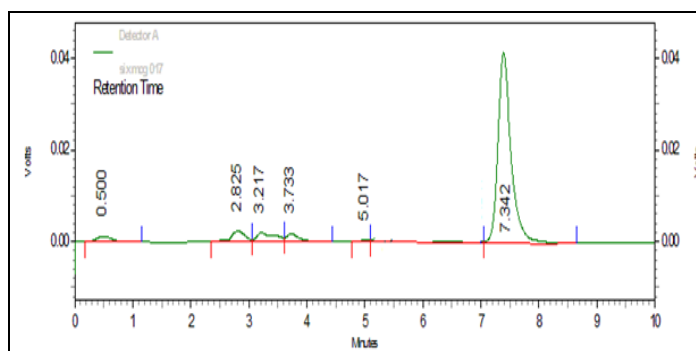


FIG. 6: REPRESENTATIVE HPLC CHROMATOGRAPH OF CURCUMIN

TABLE 4: CALIBRATION CURVE OF CURCUMIN IN PBS AT pH 7.4

S. no.	Conc. (µg/ml)	Peak area			Mean	SD	% CV= Standard deviation / Mean × 100
		N <sub>1</sub>	N <sub>2</sub>	N <sub>3</sub>			
1	2	65032.33	57192.45	61028.7	61084.43	3200.86	5.24
2	4	128974	114384.93	120564.7	121307.87	5979.10	4.92
3	6	172121.3	161576.72	169856.4	167851.47	4532.24	2.70
4	8	229087.3	238768.48	225684.8	231180.19	5542.61	2.39
5	10	284419.7	295960.6	289654.7	290011.66	4718.30	1.62
6	12	34212.2	363152.4	346548.7	352637.76	7465.92	2.11
7	14	417968.7	430344.3	414785.9	421032.96	6711.09	1.59
8	16	462410	477536.5	459865.7	466604.06	7799.86	1.67
9	18	519782	544728.8	517875.7	527462.16	12234.13	2.31
10	20	583767.7	599920.1	581476.4	588388.06	8207.85	1.39

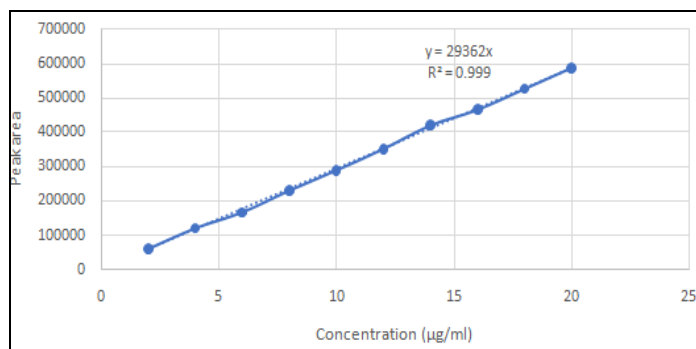


FIG. 7: CALIBRATION OF CURCUMIN BY RP- HPLC METHOD

A calibration curve was prepared using 2 - 10 µg/ml stock solution to determine the linearity of the proposed method. The retention time of curcumin was found by  $7.34 \pm 0.1$  min. The chromatogram showed good peak symmetry with no tailing as already shown in Fig. 7. Peak area v/s concentrations were plotted to create a calibration

curve, and the regression equation was computed using the average of 3 triplicate observations with a coefficient of correlation *i.e.*,  $R^2 = 0.9998$ , the regression equation,  $y = 29362x$ , where y denotes the peak area and x denotes the concentration in g/ml, provided the mean calibration curve.

### Visual Observation:

**TABLE 5: BASED ON VISUAL OBSERVATION, THE EFFECT OF VARIOUS CHITOSAN CONCENTRATIONS IS DETERMINED**

Formulation code	Concentration of Chitosan (mg/ml)	Sub- group	Concentration of TPP (mg/ml)	Visual observation
LF-1	1.0	A	1	Clear
		B	1.5	Clear
		C	2	Without opalescent ppt.
		D	3	Without opalescent ppt.
LF-2	1.5	A	1	Without opalescent ppt.
		B	1.5	Without opalescent ppt.
		C	2	With opalescent ppt.
		D	3	Opalescent with ppt.
LF-3	1.75	A	1	Clear
		B	1.5	Without opalescent ppt.
		C	2	Without opalescent ppt.
		D	3	With opalescent ppt.
LF-4	2.0	A	1	Clear
		B	1.5	Clear
		C	2	Without opalescent ppt.
		D	3	Aggregate
LF-5	2.25	A	1	Clear
		B	1.5	Without opalescent ppt.
		C	2	Aggregate
		D	3	Aggregate

### Loading Capacity, Encapsulation Efficiency, and Percentage Yield Determination of Nanoparticles:

**TABLE 6: DRUG CONCENTRATION ON ENTRAPMENT EFFICIENCY**

The volume of CS added (ml)	Volume of TPP added (ml)	Concentration of CS (mg/ml)	Concentration of TPP (mg/ml)	The concentration of drug added (mg)	Drug: polymer ratio	EE (%)
10	5	1.75	2	17.5	1:1	$85.3 \pm 3.5$
10	5	1.75	2	35.0	2:1	$81.6 \pm 4.2$
10	5	1.75	2	52.5	3:1	$75.1 \pm 3.8$

**TABLE 7: EFFECT OF DRUG CONCENTRATION ON LOADING CAPACITY**

The volume of CS added (ml)	Volume of TPP added (ml)	Concentration of CS (mg/ml)	Concentration of TPP (mg/ml)	The concentration of drug added (mg)	Drug: polymer ratio	LC (%)
10	4	1.75	2	1.75	1:1	$43.37 \pm 2.1$
10	4	1.75	2	35.0	2:1	$70.69 \pm 1.8$
10	4	1.75	2	52.5	3:1	$63.18 \pm 1.9$

### Characterization of Nanoparticles:

**TABLE 8: CHARACTERISTICS OF THE DEVELOPED NANOPARTICLES**

Formulation	Size (d.nm)	PDI	Zeta potential (mV)	EE%	LC%
CUR-CS-NP's	171.9	0.324	-35.8	$81.6 \pm 4.2$	$70.69 \pm 1.8$

## Particle size measurement by Dynamic Light Scattering (DLS):

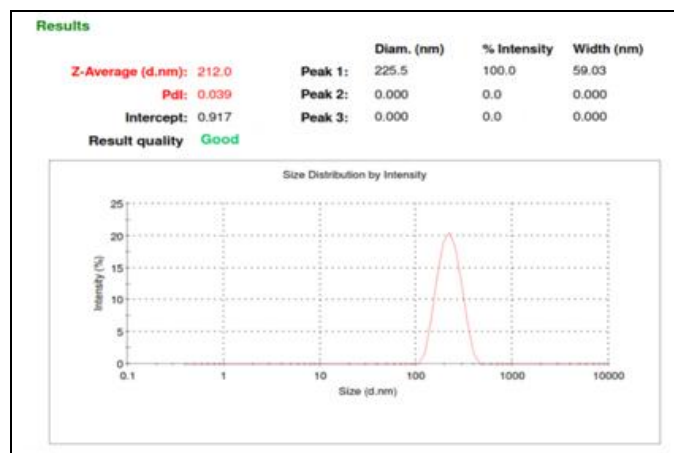
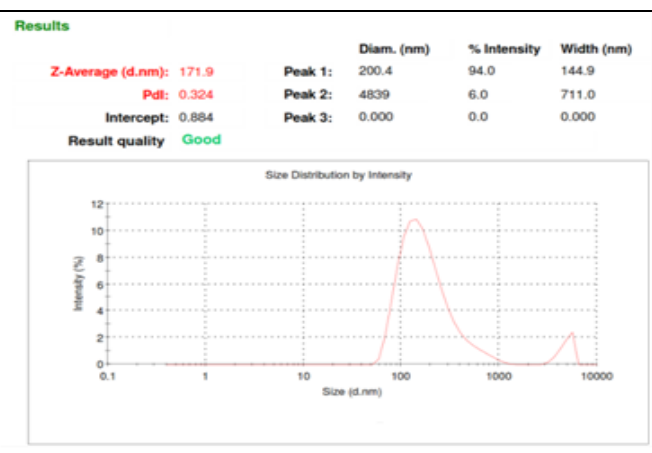
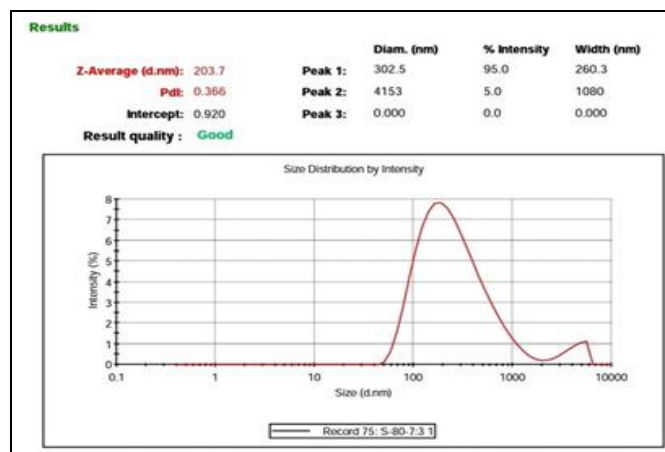
**TABLE 9: PARTICLE SIZE DISTRIBUTION AND PARTICLE SIZE OF PLACEBO FORMULATIONS**

Formulation	Concentration of CS (mg/ml)	Concentration of STPP (mg/ml)	Mean particle size (nm) ± (S.D)	Mean PDI ± (S.D)	Percentage yield ± (S.D)
LF-1C	1	2	595.5 ± 5.3	0.568 ± 0.024	48.77 ± 5.13
LF-1D	1	3	1595 ± 3.9	0.768 ± 0.013	49.77 ± 2.24
LF-2A	1.5	1	468.3 ± 6.6	0.501 ± 0.035	54.68 ± 3.56
LF-2B	1.5	1.5	193.1 ± 9.2	0.424 ± 0.012	61.45 ± 2.50
LF-3B	1.75	1.5	452.4 ± 7.2	0.466 ± 0.023	70.52 ± 3.64
LF-3C	1.75	2	109.6 ± 7.6	0.415 ± 0.065	78.98 ± 3.12
LF-4C	2	2	284.2 ± 8.6	0.611 ± 0.023	82.23 ± 2.37
LF-5B	2.25	1.5	356.6 ± 5.8	0.552 ± 0.18	88.42 ± 3.25

**TABLE 10: PARTICLE SIZE DISTRIBUTION AND PARTICLE SIZE OF THE DRUG-LOADED FORMULATION**

Formulation code	Drug: polymer ratio	Conc. of CS (mg/ml)	Conc. of TPP (mg/ml)	Mean particle size (nm) ± (S.D)	Mean PDI ± (S.D)	Percentage yield ± (S.D)
LF-21D	1:1	1.75	2	183.7 ± 8.4	0.391 ± 0.065	79.42 ± 4.62
LF-22D	2:1	1.75	2	255.4 ± 5.6	0.424 ± 0.045	82.21 ± 5.13
LF-23D	3:1	1.75	2	341.3 ± 4.7	0.462 ± 0.064	86.12 ± 4.68

**Particle size:** The particle size of the optimized NPs (LF-21D, LF-22D, and LF-23D) was estimated using a DLS instrument and has been given in **Fig. 8, 9, and 10** respectively.


**FIG. 8: PARTICLE SIZE ANALYSIS OF DRUG-LOADED FORMULATIONS**

**FIG. 9: ANALYSIS OF PARTICLE SIZE OF DRUG-LOADED FORMULATION**

**FIG. 10: ANALYSIS OF PARTICLE SIZE OF DRUG-LOADED FORMULATION**

**Zeta Potential:** Zeta potential research is a crucial component of nanoparticle characterization because surface charge plays a crucial role in enabling particle systems to adhere to biological surfaces

and ensuring the stability of suspensions. A prominent property of chitosan/TPP particles is that chitosan nanoparticles are all positively charged. The process by which particles form can be used to explain this; specifically, how positively charged -NH<sub>2</sub> groups interrelate with the negatively charged triphosphate molecules to neutralize their charges. The positive potential would be brought

on by the lingering amino groups. Chitosan nanoparticles must be more stable because they have a greater zeta potential in an optimum range. Long amino groups appear to impede anion adsorption and maintain a high electrical double layer thickness, avoiding the formation of aggregates. The zeta potential of CS-Nanoparticles is to be -35.8 mv.

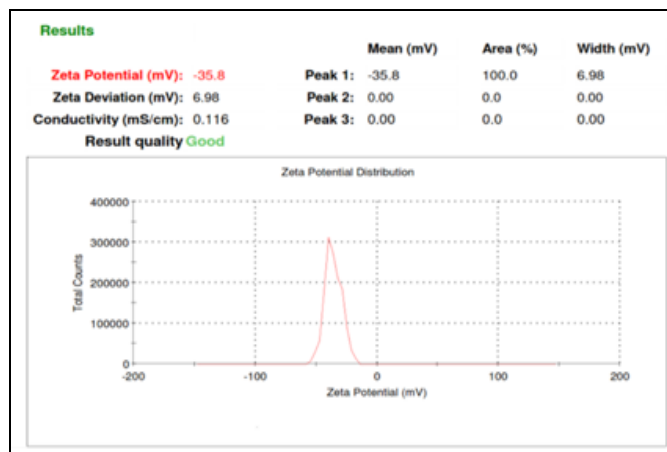


FIG. 11: ZETA POTENTIAL OF THE DRUG-LOADED FORMULATION

### Surface Morphology of Drug-loaded Chitosan Nanoparticles by TEM:

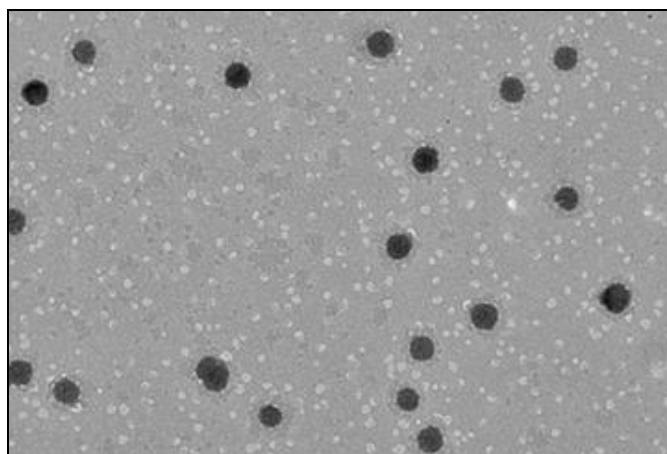


FIG. 12: TEM IMAGE OF THE OPTIMIZED CURCUMIN NANOPARTICLES

Fig. 12, which depicts TEM of the polymeric NPs, shows that the particles have sphere-shaped morphology, a smooth surface, and a size range of

about <100 nm, which is equivalent to the size determined by Dynamic Light Scattering.

### Ex-vivo Nasal Permeation Study:

TABLE 11: COMPARATIVE EX-VIVO NASAL PERMEATION STUDY

Formulation	Flux ( $\mu\text{g}/\text{cm}^2/\text{hr.}$ )	Permeability coefficient	Enhancement ratio
NP <sub>1</sub> (L21)	307.36	1.41	9.76
NP <sub>2</sub> (L22)	332.9	1.65	10.57
NP <sub>3</sub> (L23)	305.17	1.52	9.69
Control	31.495	1.47	-

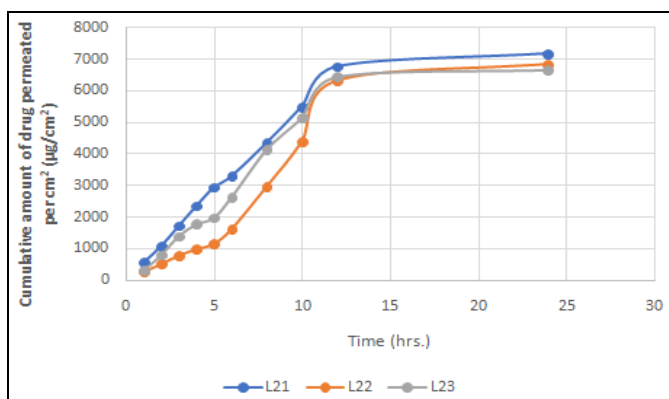


FIG. 13: *IN-VITRO* PERMEATION STUDY OF SELECTED FORMULATION

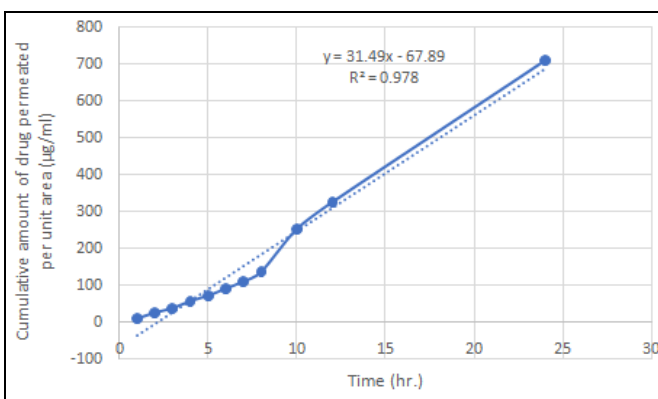


FIG. 14: PERMEATION OF CONTROL

***In-vitro* Release Profile:**

**TABLE 12: CURCUMIN DRUG RELEASE *IN-VITRO* AT pH 7.4 IN PHOSPHATE BUFFER**

Time (hr.)	Mean area n=3 (±S.D)	The cumulative amount of drug release	Cumulative % of drug release
0	0	0	0
0.5	292923.5	840	3.36
1	585847	1680	6.72
2	1129847.7	3240	12.96
4	2458465.08	7050	28.2
8	4549032.21	13045	52.18
12	7068523.02	20270	81.08
24	7499190.31	21505	86.02

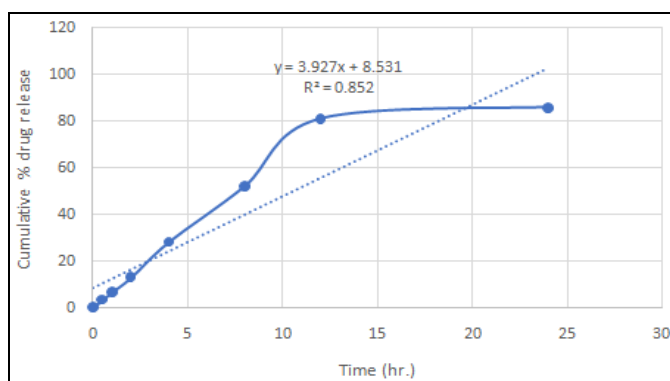


FIG. 15: CURCUMIN-LOADED CHITOSAN NANOPARTICLES RELEASED *IN-VITRO*

Fig. 15 depicts the curcumin release profile from chitosan nanoparticles. The obtained kinetic profile accounts for the existence of two distinct nanoparticle release mechanisms. Curcumin released *in vitro* demonstrated a quick initial release followed by a gradual drug release. The

first quick release of medication might be attributed to the release of curcumin from the nanoparticle surface, however later on, as a result of chitosan hydration and swelling, curcumin was regularly released from the core of nanoparticles.

**Determination of Release Rate Order:**

**Investigation of the Drug Release Profile of Drug-loaded Chitosan Nanoparticles in Phosphate Buffer at pH 7.4:**

**TABLE 13: KINETICS ANALYSIS OF CURCUMIN LOADED CHITOSAN NANOPARTICLES**

Time (min.)	The square root of time	Log time	Percentage drug release	Fraction drug release	Log % drug release	% drug remaining	Log percentage drug remaining
0	0	0	0	0	0	100	2
10	3.162	1	7.4	0.074	0.869	92.6	1.966

20	4.472	1.301	18.2	0.182	1.260	81.8	1.912
60	7.745	1.778	28.8	0.288	1.459	71.2	1.852
120	10.954	2.0769	39.1	0.391	1.592	60.9	1.784
240	15.491	2.380	49.4	0.494	1.693	50.6	1.704
480	21.908	2.681	68.2	0.682	1.833	31.8	1.502
720	26.832	2.857	83.3	0.833	1.920	16.7	1.222
1440	37.947	3.158	91.1	0.911	1.963	8.9	0.949

**In-vitro Release Kinetics Study:**

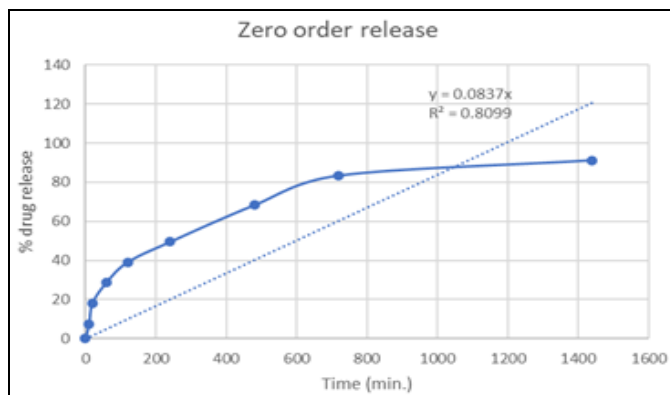


**FIG. 16: THE RELEASE PROFILE OF CURCUMIN BY ZERO ORDER RELEASE MODEL OF OPTIMIZED NANOPARTICLES**

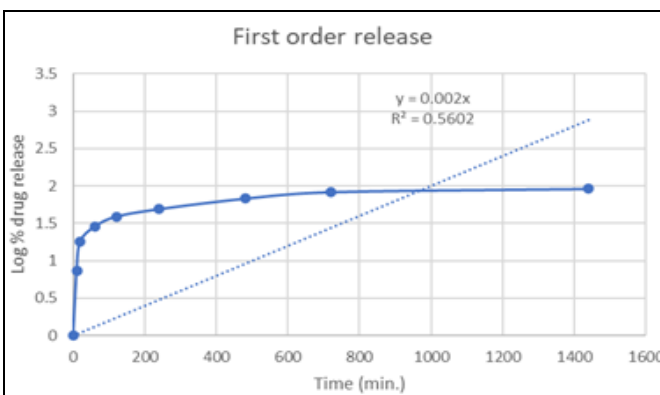


**FIG. 17: THE RELEASE PROFILE OF CURCUMIN BY FIRST ORDER RELEASE MODEL OF OPTIMIZED NANOPARTICLES**

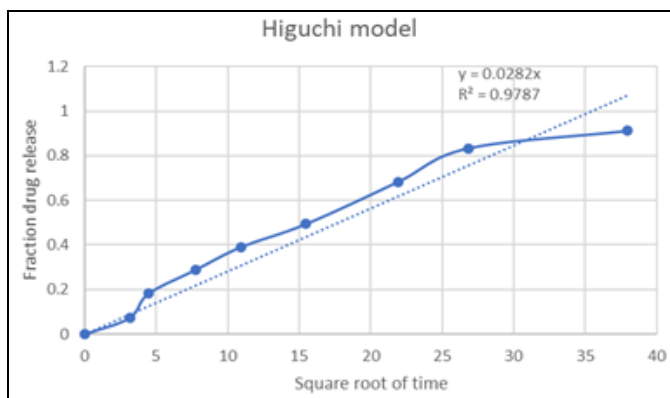


**FIG. 18: THE RELEASE PROFILE OF CURCUMIN BY HIGUCHI MODEL OF OPTIMIZED NANOPARTICLES**

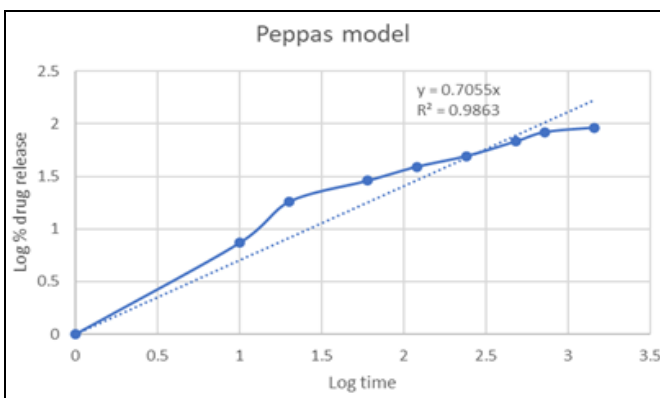


**FIG. 19: THE RELEASE PROFILE OF CURCUMIN BY THE PEPPAS MODEL OF OPTIMIZED NANOPARTICLES**

**TABLE 14: CHITOSAN NANOPARTICLES WITH AN OPTIMIZED COEFFICIENT OF CORRELATION**

Release profile model	Correlation coefficient (R <sup>2</sup> )
Zero-order model of release	0.8099
First order model of release	0.5602
Higuchi model of release	0.9787
Peppas model of release	0.9863

**Fig. 19** depicts the curcumin release profile from chitosan nanoparticles. The % drug release profile demonstrated the drug's sustained release from the formulation. Curcumin released from the *in-vitro* formulation revealed an instantaneous release for 1 hr. (greater than 30%) followed by slow drug

release for 24 hours. The first instant release of medication may be attributable to the release of Curcumin from the nanoparticle surface, whereas later on, as a result of chitosan hydration and swelling, curcumin may be constantly release from the core of nanoparticles. To determine release order, a kinetic analysis of the in-vitro profile of the optimized chitosan nanoparticles was performed. Because the correlation coefficient (R<sup>2</sup>) for the Peppas model of release was closer to unity, that is, (0.9863) for curcumin-loaded chitosan nanoparticles, the Peppas model was the best fit model for chitosan nanoparticles.

The Peppas equation was used to assess the release data, revealing a range of 0.43 to 0.85 for the release exponent 'n'. This suggests that drug release was governed by a combination of swelling and diffusion, also known as anomalous transport.

**CONCLUSION:** The drug curcumin was freely soluble in methanol. The melting point was reported to be 183°C which was in accordance with the literature cited value *i.e.*, 183°C. The calibration curve of curcumin in PBS with pH 7.4 shows an R<sup>2</sup> value of 0.9895 at 425 nm. HPLC of curcumin was carried out using water: methanol: 2-propanol with the rate of flowing 1ml/min and retention time reported to be 7.34 ± 0.1 min.

The DSC thermogram of curcumin indicated an endothermic peak at 178.152°C and a melting point of 183°C. The selected optimum formulation which depends on visual observation is further evaluated for particle size, percentage yield, entrapment efficiency (EE), drug loading (LC), surface morphology, *in-vitro* release models, and *ex-vivo* permeation studies. The average size of Curcumin-loaded CS NPs was found to be 183.7 ± 8.4nm (LF-21D), 255.4 ± 5.6nm (LF-22D), and 341.3 ± 4.7nm (LF-23D). The EE and LC were found to be 81.6 ± 4.2 and 70.69 ± 1.8 respectively, for the drug: polymer ratio (2:1). *In-vitro* kinetic investigation of the optimized chitosan NPs was done to determine release order. The Peppas model was the best appropriate model for CS-NP's because its correlation coefficient (R<sup>2</sup>) was closer to unity, that is (0.9863) for curcumin-loaded CS NPs. The Peppas equation was used to analyze the release data, and the results indicated that both swelling and diffusion- *i.e.*, anomalous transport- were responsible for controlling the drug release. The release exponent, or "n", ranged from 0.43-0.85. The maximum flux in the nasal permeation of curcumin from nanoparticle NP<sub>2</sub> (L22) is to be 332.9 µg/cm<sup>2</sup>/hr. as compared to the flux of control *i.e.*, 31.495 µg/cm<sup>2</sup>/hr. The enhancement ratio of the curcumin nanoparticle formulation (L21, L22, and L23) was found to be 9.76, 10.57, and 9.69 respectively. The Arrhenius method and ICH guidelines were followed in the accelerated stability study of Cur-NP, and a shelf life of 1.58 years was obtained. We can therefore reach the conclusion that the optimized Curcumin nanoparticles were resistant to physical stress.

As a result, sustained release formulations for intranasal delivery systems were shown to be potentially effective.

**ACKNOWLEDGMENTS:** We would like to express our gratitude to our supervisor, participants, institution, and families and friends for their support throughout this research project. Our supervisor's guidance and feedback were invaluable, and the participants' contributions were essential to the success of this study. The resources and facilities provided by our institution were crucial to the smooth execution of our research.

**CONFLICTS OF INTEREST:** There is no any conflict of interest among the authors.

## REFERENCES:

1. Aditya NP, Hamilton IE & Norton IT: Amorphous nano-curcumin stabilized oil in water emulsion: Physico chemical characterization. *Food Chemistry* 2017; 224: 191–200.
2. Hu Q & Luo Y: Chitosan-based nanocarriers for encapsulation and delivery of curcumin: A review. In *International Journal of Biological Macromolecules Elsevier B V* 2021: 125–135.
3. Huo X, Zhang Y, Jin X, Li Y & Zhang L: A novel synthesis of selenium nanoparticles encapsulated PLGA nanospheres with curcumin molecules for the inhibition of amyloid β aggregation in Alzheimer's disease. *Journal of Photochemistry and Photobiology B: Biology* 2019; 190: 98–102.
4. Wen MM, El-Salamouni NS, El-Refaie WM, Hazzah HA, Ali MM, Tosi G, Farid RM, Blanco-Prieto MJ, Billa N & Hanafy AS: Nanotechnology-based drug delivery systems for Alzheimer's disease management: Technical, industrial, and clinical challenges. In *Journal of Controlled Release Elsevier B. V* 2017; 245: 95–107.
5. Yavarpour-Bali H, Pirzadeh M & Ghasemi-Kasman M: Curcumin-loaded nanoparticles: A novel therapeutic strategy in treatment of central nervous system disorders. In *International Journal of Nanomedicine* 2019; 4449-4460.
6. Tomeh MA, Hadianamrei R and Zhao X: *Int J Mol Sci* 2019; 20: 1033.
7. Nishiga M, Wang DW, Han Y, Lewis DB and Wu JC: COVID-19 and cardiovascular disease: from basic mechanisms to clinical perspectives. *Nature Reviews Cardiology* 2020; 17: 543–558.
8. Pala R, Anju VT, Dyavaiah M, Busi S and Nauli SM: Nanoparticle-Mediated Drug Delivery for the Treatment of Cardiovascular Diseases. *International Journal of Nanomedicine* 2020; 15: 3741-3769.
9. Fan C, Joshi J, Li F, Xu B, Khan M, Yang J and Zhu W: Nanoparticle-Mediated Drug Delivery for Treatment of Ischemic Heart Disease. *Frontiers in Bioengineering and Biotechnology* 2020; 8: 687.
10. Hesari M, Mohammadi P, Khademi F, Shackebaei D, Momtaz S, Moasefi N, Farzaei MH and Abdollahi M: Current Advances in the Use of Nanophytomedicine Therapies for Human Cardiovascular Diseases.

- International Journal of Nanomedicine 2020; 16: 3293-3315.
11. Shah SMA, Akram M, Riaz M, Munir N and Rasool G: Cardioprotective Potential of Plant-Derived Molecules: A Scientific and Medicinal Approach. Dose-response: a publication of International Hormesis Society 2019; 17 (2): 1598.
  12. Thakur S, Kaurav H and Chaudhary G: Terminalia arjuna: A Potential Ayurvedic Cardio Tonic. Inter J for Research in Applied Sciences and Biotechn 2021; 8(2): 227- 236.
  13. Xiao-Huan Zhang, Chong-Yong Li, Qing-Hua Lin, ZhiHeng He, Feng Feng and Ming-Fang He: Pro-angiogenic activity of isoliquiritin on HUVECs in vitro and zebrafish *in-vivo* through Raf/MEK signaling pathway. Life Sciences 2019; 223: 128-136.
  14. Patel RV, Mistry BV, Shinde SK, Syed R, Singh V and Han-Seung Shin: Therapeutic potential of quercetin as a cardiovascular agent. European Journal of Medicinal Chemistry 2018; 155: 889-904.
  15. Ahmed Q, Gupta N, Kumar A and Nimesh S: Antibacterial efficacy of silver nanoparticles synthesized employing Terminalia arjuna bark extract. Artificial Cells, Nanomedicine and Biotechnology 2017; 45(6): 1192-1200.
  16. Mahaman YA, Huang F, Wu M, Wang Y, Wei Z, Bao J, Salissou MT, Ke D, Wang Q, Liu R and Wang JZ: Moringa oleifera alleviates homocysteine-induced Alzheimer's Disease-like pathology and cognitive impairments. J of Alzheimers Disease 2018; 63(3): 1141-59.
  17. Nakhband A, Eskandani M, Saeedi N, Ghafari S, Omidi Y, Barar J and Garjani A: Marrubiin-loaded solid lipid nanoparticles' impact on TNF- $\alpha$  treated umbilical vein endothelial cells: A study for cardioprotective effect. Colloids and Surfaces B: Biointer 2018; 164: 299-307.
  18. Rehman MU, Khan MA, Khan WS, Shafique M and Khan M: Fabrication of Niclosamide loaded solid lipid nanoparticles: In-vitro characterization and comparative in-vivo evaluation. Artificial Cells, Nanomedicine, and Biotechnology 2018; 46(8): 1926-34.
  19. Sandhir R, Yadav A, Sunkaria A and Singhal N: Nanoantioxidants: an emerging strategy for intervention against neurodegenerative conditions. Neurochemistry International 2015; 89: 209-26.
  20. Moritz MG and Moritz M: Solid lipid nanoparticles as attractive drug vehicles: Composition, properties and therapeutic strategies. Materials Science and Engineering 2016; 68: 982-94.
  21. Lin CH, Chen CH, Lin ZC and Fang JY: Recent advances in oral delivery of drugs and bioactive natural products using solid lipid nanoparticles as the carriers. Journal of Food and Drug Analysis 2017; 25: 219-34.
  22. Doktorovová S, Kováčević AB, Garcia ML and Souto EB: Preclinical safety of solid lipid nanoparticles and nanostructured lipid carriers: Current evidence from in vitro and in vivo evaluation. European Journal of Pharmaceutics and Biopharmaceutics 2016; 108: 235-52.
  23. Baek JS and Cho CW: A multifunctional lipid nanoparticle for co-delivery of paclitaxel and curcumin for targeted delivery and enhanced cytotoxicity in multidrug-resistant breast cancer cells. Oncotarget 2017; 8: 30369-82.

**How to cite this article:**

Mangal L, Kaushik N and Alam S: Formulation and evaluation of curcumin-loaded chitosan nanoparticles and its intranasal efficacy for CNS delivery. Int J Pharm Sci & Res 2023; 14(12): 5916-29. doi: 10.13040/IJPSR.0975-8232.14(12).5916-29.

All © 2023 are reserved by International Journal of Pharmaceutical Sciences and Research. This Journal licensed under a Creative Commons Attribution-NonCommercial-ShareAlike 3.0 Unported License.

This article can be downloaded to **Android OS** based mobile. Scan QR Code using Code/Bar Scanner from your mobile. (Scanners are available on Google Playstore)